Ethanol-induced impairment in the biosynthesis of N-linked glycosylation

Welti, Michael ; Hülsmeier, Andreas J

Abstract: Deficiency in N-linked protein glycosylation is a long-known characteristic of alcoholic liver disease and congenital disorders of glycosylation. Previous investigations of ethanol-induced glycosylation deficiency demonstrated perturbations in the early steps of substrate synthesis and in the final steps of capping N-linked glycans in the Golgi. The significance of the biosynthesis of N-glycan precursors in the endoplasmic reticulum, however, has not yet been addressed in alcoholic liver disease. Ethanol-metabolizing hepatoma cells were treated with increasing concentrations of ethanol. Transcript analysis of genes involved in the biosynthesis of N-glycans, activity assays of related enzymes, dolichol-phosphate quantification, and analysis of dolichol-linked oligosaccharides were performed. Upon treatment of cells with ethanol, we found a decrease in the final N-glycan precursor Dol-PP-GlcNAc2 Man9 Glc3 and in C95- and C100-dolichol-phosphate levels. Transcript analysis of genes involved in N-glycosylation showed a 17% decrease in expression levels of DPM1, a subunit of the dolichol-phosphate-mannose synthase, and a 8% increase in RPN2, a subunit of the oligosaccharyl transferase. Ethanol treatment decreases the biosynthesis of dolichol-phosphate. Consequently, the formation of N-glycan precursors is affected, resulting in an aberrant precursor assembly. Messenger RNA levels of genes involved in N-glycan biosynthesis are slightly affected by ethanol treatment, indicating that the assembly of N-glycan precursors is not regulated at the transcriptional level. This study confirms that ethanol impairs N-linked glycosylation by affecting dolichol biosynthesis leading to impaired dolichol-linked oligosaccharide assembly. Together our data help to explain the underglycosylation phenotype observed in alcoholic liver disease and congenital disorders of glycosylation.

DOI: https://doi.org/10.1002/jcb.24713

Article

Ethanol-Induced Impairment in the Biosynthesis of N-Linked Glycosylation†

Michael Welti and Andreas J. Hülsmeier*

Institute of Physiology, University of Zürich, Zürich, Switzerland.

* correspondence to: Andreas J. Hülsmeier, Institute of Physiology, University of Zürich, Winterthurerstrasse 190, CH-8057 Zürich, Switzerland.

Phone: +41-44-635-5104. Fax: +41-44-635-6814. E-mail: a.j.hulsmeier@access.uzh.ch

Received 7 October 2013; Revised 29 October 2013; Accepted 7 November 2013
Journal of Cellular Biochemistry

DOI 10.1002/jcb.24713

Abstract

Deficiency in N-linked protein glycosylation is a long-known characteristic of alcoholic liver disease and congenital disorders of glycosylation. Previous investigations of ethanol-induced glycosylation deficiency demonstrated perturbations in the early steps of substrate synthesis and in the final steps of capping N-linked glycans in the Golgi. The significance of the biosynthesis of N-glycan precursors in the endoplasmic reticulum, however, has not yet been addressed in alcoholic liver disease. Ethanol-metabolizing hepatoma cells were treated with increasing concentrations of ethanol. Transcript analysis of genes involved in the biosynthesis of N-glycans, activity assays of related enzymes, dolichol-phosphate quantification, and analysis of dolichol-linked oligosaccharides were performed. Upon treatment of cells with ethanol, we found a decrease in the final N-glycan precursor Dol-PP-$GlcNAc_2Man_9Glc_3$ and in C95- and C100-dolichol-phosphate levels. Transcript analysis of genes involved in N-glycosylation showed a 17% decrease in expression levels of DPM1, a subunit of the dolichol-phosphate-mannose synthase, and a 8% increase in RPN2, a subunit of the oligosaccharyl transferase. Ethanol treatment decreases the biosynthesis of dolichol-phosphate. Consequently, the formation of N-glycan precursors is affected, resulting in an aberrant precursor assembly. Messenger RNA levels of genes involved in N-glycan biosynthesis are slightly affected by ethanol treatment, indicating that the assembly of N-glycan precursors is not regulated at the transcriptional level. This study confirms that ethanol impairs N-linked glycosylation by affecting dolichol biosynthesis leading to impaired dolichol-linked oligosaccharide assembly. Together our data help to explain the underglycosylation phenotype observed in alcoholic liver disease and congenital disorders of glycosylation.

Keywords

N-linked glycosylation, congenital disorder of glycosylation, alcoholic liver disease, dolichol, dolichol-linked oligosaccharides

Abbreviations

ALD, alcoholic liver disease; CDG, congenital disorder of glycosylation; CDT, carbohydrate-deficient transferrin; Dol-P, dolichol-phosphate; Dol-PP, dolichol-pyrophosphate; DPM1-3, dolichol-phosphate-mannose synthase subunits 1-3; RPN2, ribophorin 2; Glc, glucose; GlcNAc, N-acetylglucosamine; Man, mannose; ADH, alcohol dehydrogenase; CYP2E1; cytochrome P450 2E1

Introduction

Alcoholic liver disease (ALD) displays a broad spectrum of symptoms reflecting the diverse functions of the liver. Among the most prominent characteristics of ALD are fatty liver, hepatitis, and liver fibrosis. Hepatocytes are responsible for detoxification in the liver and thus for alcohol metabolism. Major metabolic changes in hepatocytes occur due to the constant need for ethanol oxidation. Ethanol conversion to acetate leads to a shift in the NAD/NADH ratio impairing glycolysis and lipolysis and initiating fatty acid synthesis. The inversion of glycolytic flux eventually results in alcoholic fatty liver [Purohit et al., 2009]. Oxidative stress is evoked by reactive oxygen species from ethanol breakdown in hepatocytes and toll-like receptor 4 activation by LPS leaking from the gut into the blood stream [Wang et al., 2012; Zhu et al., 2012]. This oxidative stress contributes to liver inflammation and can lead to liver fibrosis and eventually cirrhosis. Another clinical feature in ALD receiving less attention is alcohol-induced deficiency in N-linked protein glycosylation although it has been used as a marker for alcohol abuse [Stibler, 1991].

ALD and congenital disorders of glycosylation (CDG) share some symptoms. Typically, CDG display systemic deficiencies like psychomotor retardation with variable neuromuscular involvement and additional features like hormonal abnormalities and coagulopathies [Leroy, 2006]. Importantly, fatty liver, hepatitis, and liver fibrosis are also found in CDG indicating a possible role of glycosylation in ALD pathology. Indeed, CDG was linked to a fibrotic response in fibroblasts involving the insulin-like growth factor-binding protein 5 [Lecca et al., 2011]. As in CDG, blood serum proteins originating from the liver are not glycosylated properly in ALD. For instance, the distribution of carbohydrate-deficient transferrin (CDT) glycoforms found in ALD and CDG are similar [Bean and Peter, 1993; de Jong et al., 1992; Petren et al., 1987; Vigo and Adair, 1982]. The two glycosylation sites of transferrin are normally occupied with carbohydrates adding up to four branches carrying terminal sialic acids. Besides tetrasialo-transferrin, disialo-transferrin is the most prevalent glycoform of transferrin in blood serum. In ALD and CDG, asialo- and disialo-transferrin become more apparent and tetrasialo-transferrin levels are reduced [Hülsmeier et al., 2007]. In CDG, such a CDT pattern indicates a deficiency in the assembly of the N-linked glycan precursor in the ER [Filipovic and Menzel, 1981].

So far, glycosylation deficiency in ALD has been assessed at the levels of Golgi glycosylation and dolichol metabolism. However, N-linked glycosylation starts in the ER and requires the synthesis of an oligosaccharide precursor on dolichol-phosphate (Dol-P). On the outer leaflet of the ER, one phospho-GlcNAc, one GlcNAc, and five Man are sequentially transferred to Dol-P before flipping the resulting Dol-PP-$GlcNAc_2$-Man_5 into the ER lumen. After the addition of four Man and three Glc residues, the complete N-glycan precursor, Dol-PP-$GlcNAc_2$-Man_9-Glc_3 is transferred *en bloc* to target proteins. Microsomes isolated from rat livers of chronically ethanol-fed animals showed a decrease in total dolichol by 36% [Cottalasso et al., 1998; Cottalasso et al., 1996]. Acute treatment with ethanol of rats resulted in a reduction of total dolichol in liver microsomes by up to 52%. In a cell culture model, HepG2 cells treated with 50-100 mM ethanol showed decreased transcription of the α2,6-sialyltransferase[Garige et al., 2006; Garige et al., 2005; Rao and Lakshman, 1997; Rao and Lakshman, 1999]. This enzyme is responsible for terminal sialylation of sugar chains of transferrin in the Golgi apparatus. The same effect was observed in the liver from chronically ethanol-fed rats. Additionally, the α2,6-sialyltransferase mRNA is destabilized by a 3'-untranslated region-specific binding protein. Notably, besides downregulation of α2,6-sialyltransferase other effects could cause CDT. Several intermediates along the biosynthesis of the N-glycan precursor might be affected, potentially leading to an altered distribution of glycoforms. In one study the site occupancy of serum protein glycosylation in an alcohol abusing subject was reported to be reduced to levels observed in patients with mild forms of CDG [Hülsmeier et al., 2007]. Another study reported the loss of one or both N-glycans as the cause for CDT in patients with severe alcohol abuse [Peter et al., 1998].

To understand the mechanisms underlying alcohol-induced glycosylation deficiency, we investigated the effects of ethanol exposure on the early steps of N-linked protein glycosylation in two cell models. Cultured hepatocytes usually lose the expression of drug metabolizing enzymes [Carter and Wands, 1988; Gapp et al., 2012; Luo et al., 2006; Utesch et al., 1992; Van Kaick et al., 1983]. Therefore, we used two cell lines expressing ethanol metabolizing enzymes in our study. First, the HepaRG cell line derived from a human hepatocellular carcinoma with an inducible cytochrome p450 system which renders the cell line suitable as a model for metabolism of xenobiotics in the human liver [Crick and Carroll, 1987; Eggens et al., 1990; Eggens

and Elmberger, 1990; Keller, 1986; Stoll et al., 1988; Yokoyama et al., 1989]. Ethanol degradation via cytochrome p450 2E1 (CYP2E1) is a major pathway of ethanol metabolism and can be induced by DMSO treatment in HepaRG cells [Koop and Tierney, 1990; Lieber, 1999; Ohnishi and Lieber, 1977]. The second cell line, VA-13, is derived from HepG2 cells, which expresses murine alcohol dehydrogenase 1 (ADH) [Clemens et al., 2002]. Ethanol degradation via alcohol dehydrogenase is the second major pathway of ethanol metabolism in the liver. We tested the effect of ethanol metabolism in hepatocytes on the N-linked glycosylation pathway in the ER and found that N-linked glycosylation is affected at several stages along the biosynthetic pathway.

Materials and Methods

Cell lines and experimental conditions

HepaRG cells were kindly provided by Dr. N. Zitzmann (Department of Biochemistry, University of Oxford, UK). HepaRG cells were seeded at a density of 2.6 x 10^4 cells/cm^2 and cultured in Williams' Medium E (Sigma-Aldrich) supplemented with 10% FBS, 5 μg/ml insulin, 2 mM L-glutamine, and 50 μM hydrocortisone hemisuccinate for two weeks. To induce maximal induction of the P450 enzymes, HepaRG cells were cultured for two additional weeks in the same medium added with 2% DMSO (Sigma) [Gripon et al., 2002]. On day 24 after seeding, ethanol was added to the medium and culture flasks were sealed with Parafilm to prevent evaporation of ethanol. HepaRG cells were harvested and analyzed after 28 days in culture. VA-13 cells were a kind gift from Dr. D.L. Clemens (Department of Internal Medicine, University of Nebraska Medical Center, USA). VA-13 cells are HepG2 cells stably transfected with an expression plasmid carrying the murine alcohol dehydrogenase gene, Adh-1 [Clemens et al., 2002]. VA-13 cells were seeded at a density of 1.7 x 10^4 cells/cm^2 and ethanol treatment was started 6 h after seeding. VA-13 cells were harvested and analyzed 4 days after treatment start.

Isoelectric focusing gel electrophoresis and immunoblotting

Supernatant from cultured hepatoma cells was saturated with 0.4 mM ferric citrate in presence of 20 mM sodium hydrogen carbonate for 30 min. Samples were analyzed using pre-cast Novex pH 3-7 IEF gels (Invitrogen). Gels were run at 7 mA (500 V maximum voltage) for 4 h on ice. Proteins were transferred to a nitrocellulose membrane by Western blotting. Transferrin isoforms were visualized using polyclonal rabbit anti-human transferrin primary antibody (DakoCytomation, Denmark) and peroxidase-coupled goat anti-rabbit secondary antibody (Vector Laboratories, USA).

Alcohol dehydrogenase activity assay

Alcohol dehydrogenase (ADH) activity was measured in cell lysates as previously described [Clemens et al., 1995]. Activity was determined in an assay using ethanol and NAD as substrates. ADH activity was indirectly determined from the conversion of NAD by measuring NADH photometrically at 340 nm.

Cytochrome P450 2E1 activity assay

Cytochrome p450 2E1 activity was determined as described previously [Wu and Cederbaum, 2008]. Microsomal fractions were prepared and assayed for CYP2E1 activity using *p*-nitrophenol and NADPH as substrates.

Quantitative PCR for transcript analysis

Transcript analysis of the glycosylation pathway were quantified with an adapted method for quantitative PCR in mice [Nairn et al., 2010]. Mann-Whitney statistical analysis was done using the InStat software (GraphPad). Significance was accepted for $p < 0.05$.

Dolichol-phosphate-mannose synthase activity assay

Cells were grown on 300 cm^2 plates and collected by trypsinization. Prior to cell lysis, cells were washed twice in ice-cold PBS. The cells were lysed in 25 mM Tris-HCl, 150 mM KCl, 1% Triton X-100, and cell debris was removed by centrifugation. Protein concentration was determined by BCA (Pierce). Dolichol-phosphate-mannose (Dol-P-Man) synthase activity was assayed using 30 ml of cell lysate in 100 ml of reaction buffer, with the addition of 40 mg/ml Dol-P (Sigma-Aldrich Co.) and 17 mM GDP-[^{14}C] mannose (Amersham Pharmacia Biotech). The reaction buffer contained 50 mM HEPES (pH 7.4), 25 mM KCl, 5 mM $MgCl_2$, 5 mM $MnCl_2$, and 0.2% Triton X-100. Reaction mixtures were incubated for 5 min at 37°C. Dol-P-Man was isolated by organic extraction with chloroform/methanol (2:1 vol/vol), and radioactivity was determined in a beta counter (Beckman Coulter Inc., Fullerton, California, USA) [McLachlan and Krag, 1994]. Statistical significance was determined by paired student t-test. Significance was accepted for $p < 0.05$.

Fluorescent labeling and analysis of dolichol-phosphate

Extraction, labeling, and analysis of Dol-P were adapted from previous studies [Elmberger et al., 1989; Haeuptle et al., 2010]. Briefly, approximately 3 x 10^8 cells were collected by trypsinization, counted, and washed once in PBS. For quantification, 10 μg C_{80}-polyprenol-phosphate (Larodan Fine Chemicals, Sweden) was added as internal standard. After addition of 6 ml methanol and 3 ml 15 M KOH, the sample was hydrolyzed for 1 h at 100 °C. Dolichol and Dol-P were extracted with chloroform/methanol (2:1 vol/vol) and the chloroform phase was dried under nitrogen. The sample was dissolved in methanol/water (98:2 vol/vol) supplemented with 20 mM phosphoric acid and applied to a C_{18} SepPak column (Waters, USA). Dolichol and Dol-P were eluted in chloroform/methanol (2:1 vol/vol) followed by separation on a Silica SepPak column

(Waters, USA). Dol-P was eluted in chloroform/methanol/water (10:10:3 vol/vol/vol). Dol-P was fluorescently labeled with 9-anthryldiazomethane (Sigma-Aldrich) in a multi-step procedure described elsewhere [Haeuptle et al., 2010].

Samples were analyzed by using a LaChrom D-7000 HPLC system (Merck, Germany) equipped with an Inertsil ODS-3 column (5 µm, 4.6 x 250 mm; GL Sciences Inc., Japan). Fluorescence was detected using a LaChrom L-7485 fluorescence detector using 365 nm as excitation wavelength and 412 nm as emission wavelength. Separation was done by applying isocratic elution with acetonitrile/dichloromethane (3:2 vol/vol) supplemented with 0.01% diethylamine (Sigma–Aldrich). Flow was held constant at 1 ml/min at 30 °C. Statistical analysis was done by paired student t-test. Significance was accepted for $p < 0.05$.

Radioactive labeling and analysis of dolichol-linked oligosaccharides

After ethanol exposure, cells were washed with PBS and incubated in serum- and glucose-free DMEM (Invitrogen) for 45 min at 37°C. Metabolic labeling of dolichol-linked oligosaccharide was performed by addition of 150 µCi [^{3}H]mannose (Hartmann, Germany) for 1 h at 37°C. Cells were washed twice with PBS and scraped in 11 ml methanol and 0.1 mM Tris, pH 7.4 (8:3 vol/vol). After the addition of 12 ml chloroform and vortexing, cells were pelleted by centrifugation at 5,000 x *g* for 5 min. Dolichol-linked oligosaccharides were extracted as described previously and were analyzed by HPLC [Burda et al., 1998; Zufferey et al., 1995]. The peak areas corresponding to the dolichol-linked oligosaccharides were normalized and the relative signal intensities per oligosaccharide were calculated for each run. Data were subjected to paired t-test for statistical analysis. Significance was accepted for $p < 0.05$.

Results

VA-13 and HepaRG cell lines express ethanol-metabolizing enzymes

Initially, we assessed the CYP2E1 and ADH activities in the HepaRG and VA-13 cells to confirm their validity as ethanol metabolizing cell lines. Expression of murine ADH and induction of CYP2E1 were confirmed in VA-13 and HepaRG cells, respectively. ADH activity could not be detected in naïve HepG2 cells but was present in VA-13 cells (Figure 1 A). CYP2E1 activity could be induced with 2% DMSO treatment for two

weeks in HepaRG cells (Figure 1 B). The activity of ADH and CYP2E1 was reflected in the cytotoxicity towards ethanol (Figure 1 C and D). After 4 d of ethanol treatment, viability of VA-13 cells was markedly decreased. VA-13 sensitivity towards ethanol has been previously described [Clemens et al., 2002]. Compared to rat liver microsomes, the microsomal fractions of induced HepaRG cells showed a 8.6-fold reduced activity of CYP2E1. Induced HepaRG cells showed a similar sensitivity to ethanol as the VA-13 cells and viability was reduced by 39% upon ethanol treatment.

Transferrin glycosylation is unaffected by ethanol treatment

To investigate the production of CDT, hepatocytes were exposed to different concentrations of ethanol for 4 days and supernatants were analyzed. Supernatants were subjected to isoelectric focusing and immunoblotting against transferrin. Transferrin glycoform distribution was different in supernatants of cultured hepatocytes compared to blood serum (Figure 2). In contrast to blood serum, supernatants showed more prominent asialo- up to trisialo-transferrin bands instead of tetrasialo- and disialo-transferrin, which were prominent in healthy control serum. This pattern could be observed both cell lines and reflects the aberrant N-glycosylation found in hepatic carcinoma conditions [Kamiyama et al., 2013]. Moreover, no effect on glycoform distribution was visible using concentrations between 25 to 200 mM ethanol. A potential effect on the transferrin glycoform pattern might be mild and could be masked by the hepatoma specific glycoform distribution. With using higher ethanol concentrations, less transferrin was detected. The decrease in transferrin signal reflected low cell numbers due to ethanol toxicity or may indicate impaired protein secretion. In contrast, the transferrin signal of the parental HepG2 cell line remained stable after exposure to 25 mM or 200 mM ethanol, emphasizing the need of ethanol metabolizing enzyme activity to impact protein secretion or protein glycosylation. Hepatoma cells and hepatocytes lose their ability to metabolize ethanol due to a significant decline in ADH and CYP2E1 expression during cell culture.

Transcript analysis reveals potential regulatory changes along the N-glycosylation pathway

To get more detailed information of changes occurring in the N-linked glycosylation pathway, we analyzed the transcripts of different glycosylation genes that are involved in key steps of the Dol-linked oligosaccharide assembly by quantitative PCR after 25 mM and 100 mM ethanol treatment for 4 days (Figure 3 A). No

significant changes could be observed for the analyzed transcripts upon 25 mM ethanol treatment. After treatment with 100 mM ethanol, however, the mRNA levels of two genes were slightly changed. DPM1, a subunit of DPM synthase, was downregulated by 17%. DPM synthase works as a heterotrimer (DPM1-DPM3) transferring a Man-1-P from GDP-mannose to Dol-P. The resulting Dol-P-Man serves as a substrate for mannosyl transferases in the ER lumen. The second transcript RPN2 was upregulated by 8%. RPN2 is a ribophorin taking part in the recruitment of the oligosaccharyl transferase complex to the ER-coupled ribosomes. We observed a dose dependency on ethanol concentration as a trend in all the tested transcripts. For instance, DPM1 mRNA was decreased at 25 mM ethanol but only at 100 mM ethanol the change was significant between control and ethanol-treated cells.

DPM synthase activity was measured to determine whether the lower transcript level of DPM1 would affect DPM synthase activity. We found a marked increase in DPM synthase activity in cell lysates from ethanol treated VA-13 cells (Figure 3 B). The increase in DPM synthase activity stands in contrast with the minor decrease in DPM1 transcript levels. Notably, the catalytic subunit of DPM synthase was not affected at the transcriptional level. The moderate downregulation in DPM1 transcript together with the 36% increase in DPM synthase activity might point to a regulatory mechanism.

Dolichol-phosphate pool is decreased after ethanol treatment

Next, we assessed the most prevalent Dol-P species consisting of 90, 95, and 100 carbon atoms in hepatoma cells. Treatment of HepaRG cells with ethanol resulted in a decrease of Dol-P levels (Figure 4). The strongest decrease was detected for the C95-Dol-P, which was reduced by 80% whereas C100-Dol-P was decreased by 64% in comparison to untreated cells (Figure 4 C).

N-glycan precursor assembly is impaired after ethanol treatment

In CDG types that affect the biosynthesis of the N-glycan precursor, different intermediate dolichol-linked oligosaccharides can accumulate. To address ethanol-induced changes in N-glycan precursor assembly, we metabolically labeled dolichol-linked oligosaccharides with [^{3}H]mannose and subsequently separated them by HPLC coupled to a flow scintillation analyzer. The dolichol-linked oligosaccharide profile underwent a shift, displaying a smaller fraction of the final oligosaccharide precursor when cells were treated with 100 mM ethanol (Figure 5 A , B). A reduction of the $GlcNAc_2$-Man_9-Glc_3 peak by 27% was observed in HepaRG cells

indicating either a lower availability of dolichol leading to a general decrease is dolichol-linked oligosaccharide or a defect in a later stage of the N-glycan biosynthesis in the ER. Typically, defects more early in the biosynthesis lead to an accumulation or a uniform decrease of dolichol-linked oligosaccharide precursors (Figure 5 C). The same trend of a reduced $GlcNAc_2$-Man_9-Glc_3 peak could be observed in VA-13 cells (Figure 5 D).

Discussion

We investigated the effect of ethanol exposure on N-linked protein glycosylation and observed lower Dol-P levels, in particular C95-Dol-P in our HepaRG model. Lower dolichol levels have been reported previously in murine model systems upon ethanol treatment [Cottalasso et al., 1998; Cottalasso et al., 1996]. Dol-P is critical for N-glycosylation in two ways. First, it serves as a carrier for the N-glycan precursor. Second, Dol-P coupled to Man or Glc is essential for glycosyltransferases located in the ER lumen. Accordingly, low availability of Dol-P-Man in DPM1-CDG was previously demonstrated to be attenuated by increasing Dol-P thereby compensating the low activity of DPM synthase with better substrate availability [Haeuptle et al., 2011]. The strategy of increasing dolichol levels to attenuate glycosylation deficiency in ALD would be interesting but might not be sufficient due to the complexity of ethanol-induced N-glycosylation deficiency.

This is the first study showing ethanol-induced effects on the biosynthesis of the N-glycan precursors, namely a reduction of Dol-PP-$GlcNAc_2Man_9Glc_3$ compared to untreated cells. Interestingly, while general decrease in dolichol-linked oligosaccharide is well defined in CDG, such a reduction of the final dolichol-linked precursor has not been observed yet, neither in inherited nor in acquired glycosylation deficiencies. The dolichol-linked oligosaccharide pattern suggests a deficiency in the ER luminal assembly of the N-glycan precursor or could be a consequence of lower dolichol levels. CDG research has shown that deficient enzymes of the early, cytosolic steps of N-glycan precursor biosynthesis preferentially lead to an accumulation of Dol-P precursors, such as Dol-PP-$GlcNAc_2$-Man_5 in DPM1-CDG [Imbach et al., 2000]. The shortage in dolichol could also explain the lower Dol-PP-$GlcNAc_2Man_9Glc_3$ levels with decreased availability of the N-glycan precursors, leading to drainage of the dolichol-linked oligosaccharide pool. CDG with deficient dolichol or Dol-P biosynthesis

typically result in reduced dolichol-linked oligosaccharide but do not alter the distribution of the dolichol-linked precursors as observed in DOLK-CDG [Kranz et al., 2007]. In SRD5A3-CDG, the polyprenol reductase along the dolichol biosynthetic pathway is non-functional but does not lead to decreased dolichol levels and fibroblasts show a healthy dolichol-linked oligosaccharide distribution [Grundahl et al., 2012]. Symptoms on the systemic level are not shared by CDG affecting dolichol biosynthesis and ALD. The tendency of CDG for liver malformation or disease is apparent in other forms of CDG with defects in later steps of the N-linked glycosylation pointing towards a more complex mechanism in N-glycosylation deficiency in ALD.

Transcriptional regulation of N-glycosylation genes could explain ethanol-induced N-glycosylation deficiency. We found a trend for transcript alteration upon ethanol treatment but only to a marginal extent. DPM1, a subunit of the DPM synthase, was transcriptionally downregulated by 17% indicating a regulatory mechanism. This notion is supported by our observation that DPM synthase activity was increased by 36%. More work is needed to elucidate possible regulatory mechanisms for the N-glycosylation pathway in ALD. Since reduced Dol-PP-$GlcNAc_2Man_9Glc_3$ might be due to dysfunction of the later, luminal steps of the N-glycan precursor assembly, a deregulation of the oligosaccharyl transferase (OST) offers an explanation. Indeed, we found an indication for potential OST deregulation. RPN2, a part of the OST complex, was slightly upregulated. RPN2 was shown to promote glycosylation of P-glycoprotein, an ABC transporter of the multidrug resistance family [Honma et al., 2008; Kerb et al., 2001]. Knock-down of RPN2 resulted in reduced glycosylation as well as reduced membrane localization of P-glycoprotein. We speculate that RPN2 upregulation upon ethanol-treatment induces changes in N-linked glycosylation of RPN2 target proteins contributing to an aberrant dolichol-linked oligosaccharide pattern. It would be interesting to further investigate the expression and function of OST subunits in order to get a notion of the impact of ethanol on OST activity.

In conclusion, we found that decreased Dol-P and altered dolichol-linked oligosaccharide profiles contribute to ethanol-induced N-linked glycosylation deficiency. Furthermore, altered transcription of genes along the N-linked glycosylation pathway was found indicating a deregulation in N-glycosylation. Together with previous findings of lower sialyltransferase and higher sialidase activities, ethanol-induced glycosylation deficiency proves to be a result of metabolic interferences along the N-glycosylation biosynthetic pathway starting from

the early steps of dolichol synthesis, continuing with the biosynthesis of the N-linked glycan precursor, and concluding with the final steps of glycan capping in the Golgi apparatus.

Acknowledgements

We thank Drs. Alison V. Nairn and Kelley W. Moremen, Complex Carbohydrate Research Center, University of Georgia, Athens, USA for the quantitative PCR and transcript analyses. We thank Dr. N. Zitzmann, Department of Biochemistry, University of Oxford, UK and Dr. D.L. Clemens Department of Internal Medicine, University of Nebraska Medical Center, USA, for providing us with hepatoma cell lines. We are grateful to Dr. Thierry Hennet, Institute of Physiology, University of Zurich for helpful discussions and critically reading of the manuscript. This work was supported by the University of Zurich and the Swiss national science foundation, grant number 310030-129633. The authors confirm that there are no conflicts of interest.

References

Bean P, Peter JB. 1993. A new approach to quantitate carbohydrate-deficient transferrin isoforms in alcohol abusers: partial iron saturation in isoelectric focusing/immunoblotting and laser densitometry. Alcohol Clin Exp Res 17:1163-70.

Burda P, Borsig L, de Rijk-van Andel J, Wevers R, Jaeken J, Carchon H, Berger EG, Aebi M. 1998. A novel carbohydrate-deficient glycoprotein syndrome characterized by a deficiency in glucosylation of the dolichol-linked oligosaccharide. J Clin Invest 102:647-52.

Carter EA, Wands JR. 1988. Ethanol-induced inhibition of liver cell function: I. Effect of ethanol on hormone stimulated hepatocyte DNA synthesis and the role of ethanol metabolism. Alcohol Clin Exp Res 12:555-62.

Clemens DL, Forman A, Jerrells TR, Sorrell MF, Tuma DJ. 2002. Relationship between acetaldehyde levels and cell survival in ethanol-metabolizing hepatoma cells. Hepatology 35:1196-204.

Clemens DL, Halgard CM, Miles RR, Sorrell MF, Tuma DJ. 1995. Establishment of a recombinant hepatic cell line stably expressing alcohol dehydrogenase. Arch Biochem Biophys 321:311-8.

Cottalasso D, Bellocchio A, Pronzato MA, Domenicotti C, Traverso N, Gianelli MV, Marinari UM, Nanni G. 1998. Effect of ethanol administration on the level of dolichol in rat liver microsomes and Golgi apparatus. Alcohol Clin Exp Res 22:730-7.

Cottalasso D, Gazzo P, Dapino D, Domenicotti C, Pronzato MA, Traverso N, Bellocchio A, Nanni G, Marinari UM. 1996. Effect of chronic ethanol consumption on glycosylation processes in rat liver microsomes and Golgi apparatus. Alcohol Alcohol 31:51-9.

Crick DC, Carroll KK. 1987. Extraction and quantitation of total cholesterol, dolichol and dolichyl phosphate from mammalian liver. Lipids 22:1045-8.

de Jong G, van Noort WL, van Eijk HG. 1992. Carbohydrate analysis of transferrin subfractions isolated by preparative isoelectric focusing in immobilized pH gradients. Electrophoresis 13:225-8.

Eggens I, Ekstrom TJ, Aberg F. 1990. Studies on the biosynthesis of polyisoprenols, cholesterol and ubiquinone in highly differentiated human hepatomas. J Exp Pathol (Oxford) 71:219-32.

Eggens I, Elmberger PG. 1990. Studies on the polyisoprenoid composition in hepatocellular carcinomas and its correlation with their differentiation. APMIS 98:535-42.

Elmberger PG, Eggens I, Dallner G. 1989. Conditions for quantitation of dolichyl phosphate, dolichol, ubiquinone and cholesterol by HPLC. Biomed Chromatogr 3:20-8.

Filipovic I, Menzel B. 1981. Action of low-density lipoprotein and compactin, a competitive inhibitor of 3-hydroxy-3-methylglutaryl-CoA reductase, on the synthesis of dolichol-linked oligosaccharides and low-density-lipoprotein receptor in human skin fibroblasts. Biochem J 196:625-8.

Gapp IW, Congreve CR, Lieberman BS. 2012. Unraveling the phylogenetic relationships of the Eccoptochilinae, an enigmatic array of ordovician cheirurid trilobites. PLoS One 7:e49115.

Garige M, Gong M, Lakshman MR. 2006. Ethanol destabilizes liver Gal beta l, 4GlcNAc alpha2,6-sialyltransferase, mRNA by depleting a 3'-untranslated region-specific binding protein. J Pharmacol Exp Ther 318:1076-82.

Garige M, Gong M, Rao MN, Zhang Y, Lakshman MR. 2005. Mechanism of action of ethanol in the down-regulation of Gal(beta)1, 4GlcNAc alpha2,6-sialyltransferase messenger RNA in human liver cell lines. Metabolism 54:729-34.

Gripon P, Rumin S, Urban S, Le Seyec J, Glaise D, Cannie I, Guyomard C, Lucas J, Trepo C, Guguen-Guillouzo C. 2002. Infection of a human hepatoma cell line by hepatitis B virus. Proc Natl Acad Sci U S A 99:15655-60.

Grundahl JE, Guan Z, Rust S, Reunert J, Muller B, Du Chesne I, Zerres K, Rudnik-Schoneborn S, Ortiz-Bruchle N, Hausler MG, Siedlecka J, Swiezewska E, Raetz CR, Marquardt T. 2012. Life with too much polyprenol: polyprenol reductase deficiency. Mol Genet Metab 105:642-51.

Haeuptle MA, Hülsmeier AJ, Hennet T. 2010. HPLC and mass spectrometry analysis of dolichol-phosphates at the cell culture scale. Anal Biochem 396:133-8.

Haeuptle MA, Welti M, Troxler H, Hülsmeier AJ, Imbach T, Hennet T. 2011. Improvement of dolichol-linked oligosaccharide biosynthesis by the squalene synthase inhibitor zaragozic acid. J Biol Chem 286:6085-91.

Honma K, Iwao-Koizumi K, Takeshita F, Yamamoto Y, Yoshida T, Nishio K, Nagahara S, Kato K, Ochiya T. 2008. RPN2 gene confers docetaxel resistance in breast cancer. Nat Med 14:939-48.

Hülsmeier AJ, Paesold-Burda P, Hennet T. 2007. N-glycosylation site occupancy in serum glycoproteins using multiple reaction monitoring liquid chromatography-mass spectrometry. Mol Cell Proteomics 6:2132-8.

Imbach T, Schenk B, Schollen E, Burda P, Stutz A, Grunewald S, Bailie NM, King MD, Jaeken J, Matthijs G, Berger EG, Aebi M, Hennet T. 2000. Deficiency of dolichol-phosphate-mannose synthase-1 causes congenital disorder of glycosylation type Ie. J Clin Invest 105:233-9.
Kamiyama T, Yokoo H, Furukawa J, Kurogochi M, Togashi T, Miura N, Nakanishi K, Kamachi H, Kakisaka T, Tsuruga Y, Fujiyoshi M, Taketomi A, Nishimura S, Todo S. 2013. Identification of novel serum biomarkers of hepatocellular carcinoma using glycomic analysis. Hepatology 57:2314-25.
Keller RK. 1986. The mechanism and regulation of dolichyl phosphate biosynthesis in rat liver. J Biol Chem 261:12053-9.
Kerb R, Hoffmeyer S, Brinkmann U. 2001. ABC drug transporters: hereditary polymorphisms and pharmacological impact in MDR1, MRP1 and MRP2. Pharmacogenomics 2:51-64.
Koop DR, Tierney DJ. 1990. Multiple mechanisms in the regulation of ethanol-inducible cytochrome P450IIE1. Bioessays 12:429-35.
Kranz C, Jungeblut C, Denecke J, Erlekotte A, Sohlbach C, Debus V, Kehl HG, Harms E, Reith A, Reichel S, Grobe H, Hammersen G, Schwarzer U, Marquardt T. 2007. A defect in dolichol phosphate biosynthesis causes a new inherited disorder with death in early infancy. Am J Hum Genet 80:433-40.
Lecca MR, Maag C, Berger EG, Hennet T. 2011. Fibrotic response in fibroblasts from congenital disorders of glycosylation. J Cell Mol Med 15:1788-96.
Leroy JG. 2006. Congenital disorders of N-glycosylation including diseases associated with O- as well as N-glycosylation defects. Pediatr Res 60:643-56.
Lieber CS. 1999. Microsomal ethanol-oxidizing system (MEOS): the first 30 years (1968-1998)--a review. Alcohol Clin Exp Res 23:991-1007.
Luo Y, Nita-Lazar A, Haltiwanger RS. 2006. Two distinct pathways for O-fucosylation of epidermal growth factor-like or thrombospondin type 1 repeats. J Biol Chem 281:9385-92.
McLachlan KR, Krag SS. 1994. Three enzymes involved in oligosaccharide-lipid assembly in Chinese hamster ovary cells differ in lipid substrate preference. J Lipid Res 35:1861-8.
Nairn AV, dela Rosa M, Moremen KW. 2010. Transcript analysis of stem cells. Methods Enzymol 479:73-91.
Ohnishi K, Lieber CS. 1977. Reconstitution of the microsomal ethanol-oxidizing system. Qualitative and quantitative changes of cytochrome P-450 after chronic ethanol consumption. J Biol Chem 252:7124-31.
Peter J, Unverzagt C, Engel WD, Renauer D, Seidel C, Hösel W. 1998. Identification of carbohydrate deficient transferrin forms by MALDI-TOF mass spectrometry and lectin ELISABiochim Biophys Acta 1998 Aug 24;1381(3):356. Biochim Biophys Acta 1380:93-101.
Petren S, Vesterberg O, Jornvall H. 1987. Differences among five main forms of serum transferrin. Alcohol Clin Exp Res 11:453-6.
Purohit V, Gao B, Song BJ. 2009. Molecular mechanisms of alcoholic fatty liver. Alcohol Clin Exp Res 33:191-205.
Rao MN, Lakshman MR. 1997. Chronic ethanol downregulates Gal-beta-1,4GlcNAc alpha 2,6-sialyltransferase and Gal-beta-1,3GlcNAc alpha 2,3-sialyltransferase mRNAs in rat liver. Alcohol Clin Exp Res 21:348-51.
Rao MN, Lakshman MR. 1999. Chronic ethanol consumption leads to destabilization of rat liver beta-galactoside alpha2,6-sialyltransferase mRNA. Metabolism 48:797-803.
Stibler H. 1991. Carbohydrate-deficient transferrin in serum: a new marker of potentially harmful alcohol consumption reviewed. Clin Chem 37:2029-37.
Stoll J, Rosenwald AG, Krag SS. 1988. A Chinese hamster ovary cell mutant F2A8 utilizes polyprenol rather than dolichol for its lipid-dependent asparagine-linked glycosylation reactions. J Biol Chem 263:10774-82.
Utesch D, Diener B, Molitor E, Oesch F, Platt KL. 1992. Characterization of cryopreserved rat liver parenchymal cells by metabolism of diagnostic substrates and activities of related enzymes. Biochem Pharmacol 44:309-15.
Van Kaick G, Lieberman D, Lorenz D, Lorenz WJ, Luhrs H, Scheer KE, Wesch H, Muth H, Kaul A, Immich H, Wagner G, Wegener K. 1983. Recent results of the German Thorotrast study--epidemiological results and dose effect relationships in Thorotrast patients. Health Phys 44 Suppl 1:299-306.
Vigo C, Adair WL, Jr. 1982. In vivo biosynthesis of the saturated isoprene unit of dolichyl phosphate. Biosci Rep 2:835-40.
Wang HJ, Gao B, Zakhari S, Nagy LE. 2012. Inflammation in alcoholic liver disease. Annu Rev Nutr 32:343-68.
Wu D, Cederbaum AI. 2008. Development and properties of HepG2 cells that constitutively express CYP2E1. Methods Mol Biol 447:137-50.
Yokoyama K, Mizuguchi H, Araki Y, Kaya S, Ito E. 1989. Biosynthesis of linkage units for teichoic acids in gram-positive bacteria: distribution of related enzymes and their specificities for UDP-sugars and lipid-linked intermediates. J Bacteriol 171:940-6.

Zhu H, Jia Z, Misra H, Li YR. 2012. Oxidative stress and redox signaling mechanisms of alcoholic liver disease: updated experimental and clinical evidence. J Dig Dis 13:133-42.
Zufferey R, Knauer R, Burda P, Stagljar I, te Heesen S, Lehle L, Aebi M. 1995. STT3, a highly conserved protein required for yeast oligosaccharyl transferase activity in vivo. EMBO J 14:4949-60.

Figure legends

Figure 1. Ethanol-metabolizing enzyme activities and viability in VA-13 and HepaRG cell lines. VA-13 cells were seeded at 16.7 x 10^3 cells per cm^2 and cultured for 4 days previous to ADH activity measurement (A). HepaRG cells were treated as described in Materials and Methods and CYP2E1 activity was tested in microsomal proteins of induced and un-induced cells (B). Viable cell count was determined after treatment with 100 mM ethanol for 4 days (C and D).

Figure 2. Carbohydrate-deficient transferrin as marker for glycosylation deficiency. Transferrin was analyzed 4 days after ethanol exposure using isoelectric focusing and subsequent immunoblotting. As a comparison, blood serum from a phosphomannomutase 2-CDG patient was analyzed by the same procedure.

Figure 3. Transcript analysis of the glycosylation pathway in the ER and DPM synthase activity after 100 mM ethanol treatment. Transcript analysis was performed from RNA of VA-13 cells treated with 25 or 100 mM ethanol for 4 days (A). Results are shown as mean ± SEM of four independent samples. *, $p < 0.05$. Enzyme activity was determined using cell lysates from treated or untreated VA-13 cells in an assay using C95-Dol-P as acceptor and radioactive GDP-[^{3}H]mannose as donor substrate (B). The radioactivity of labeled C95-Dol-P-Man was quantified by liquid scintillation counting. Activities shown as mean ± SEM of six independent experiments. *, $p < 0.05$.

Figure 4. Dolichol-phosphate levels after 100 mM ethanol treatment. Dol-P levels were determined in HepaRG cells after 4 d of ethanol treatment. C90, C95, and C100 peaks were identified using Dol-P standards and quantitative determination was done with using C80-Dol-P as internal standard. Representative HPLC profiles are shown (A, B). Peak areas were determined and analyzed (C). Data represent mean values ±SEM of three independent experiments. *, $p < 0.05$.

Figure 5. Dolichol-linked oligosaccharide analysis. VA-13 and HepaRG cells were metabolically labeled with [^{3}H]mannose to analyze dolichol-linked oligosaccharide precursors. Representative control and 100 mM ethanol treated sample profiles are shown (A and B). Relative peak areas of the $GlcNAc_2Man_9Glc_3$ to total area were calculated (C and D). Data represent mean values ±SEM of three independent experiments. *, $p < 0.05$.

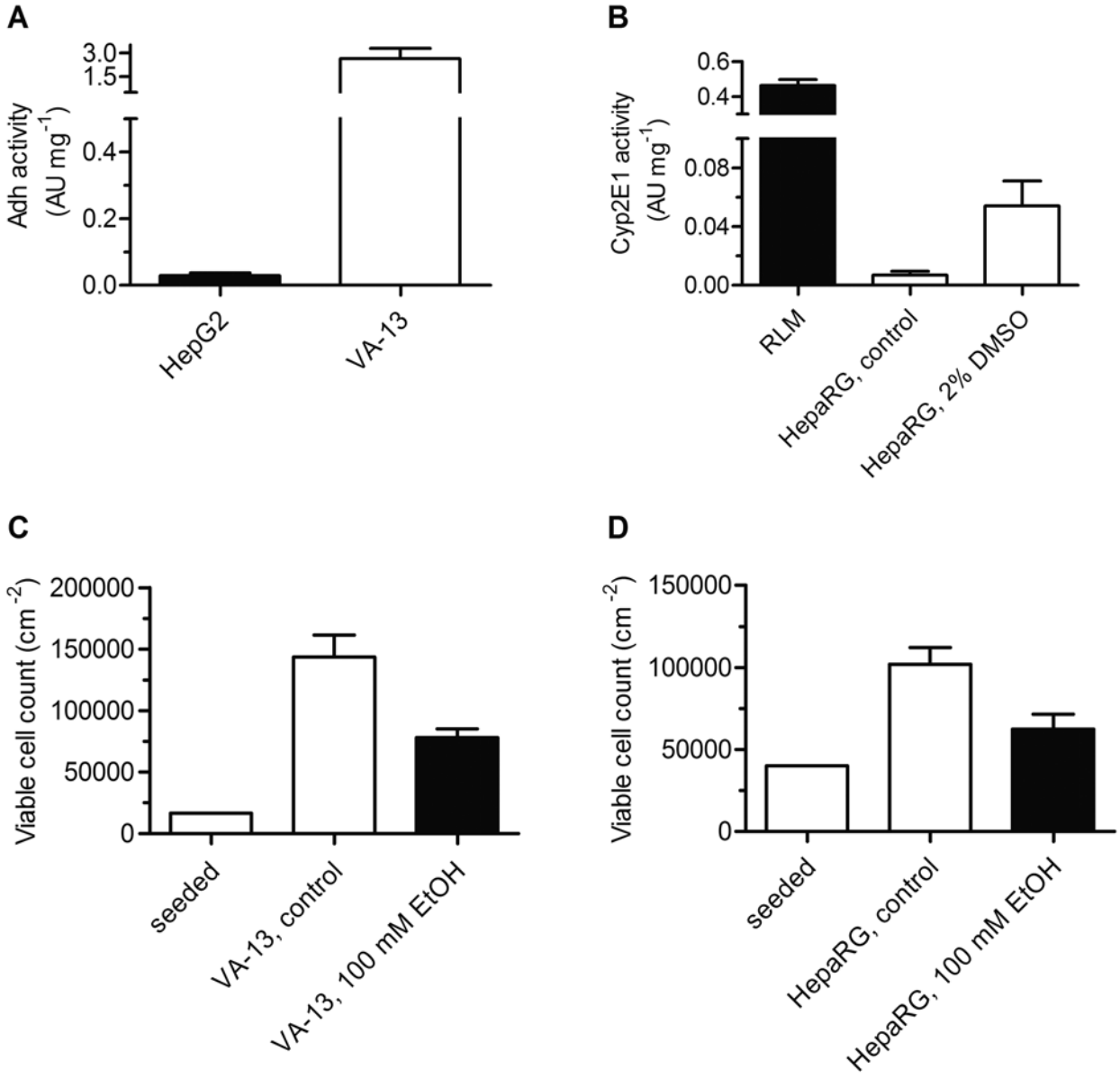

Figure 1

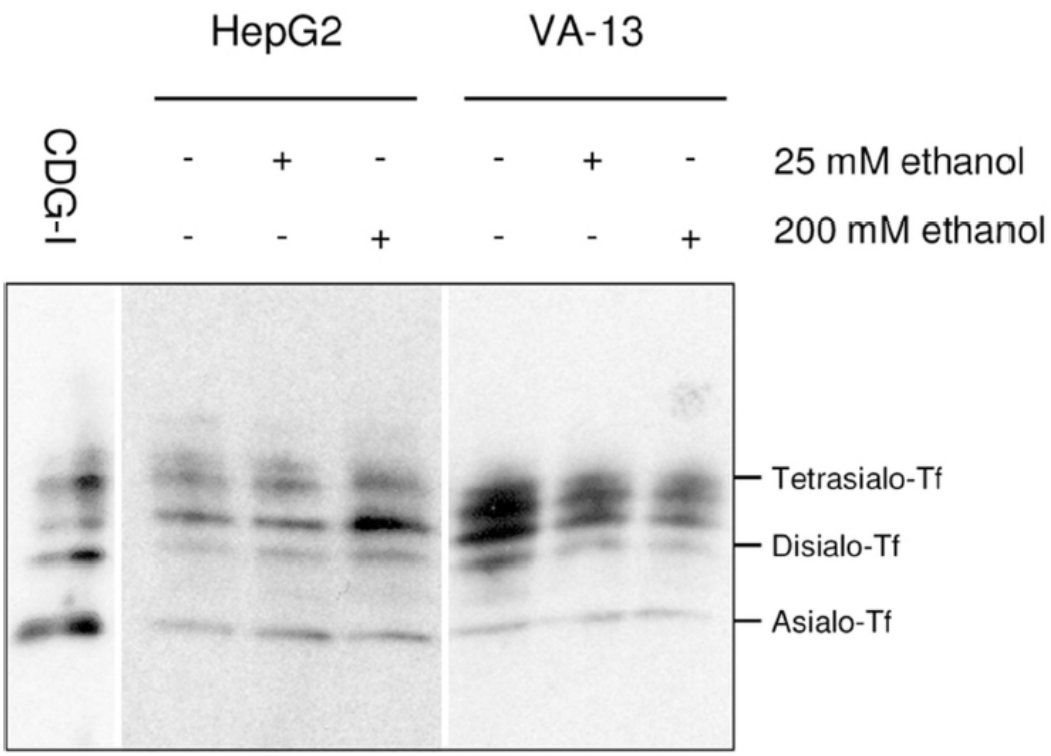

Figure 2

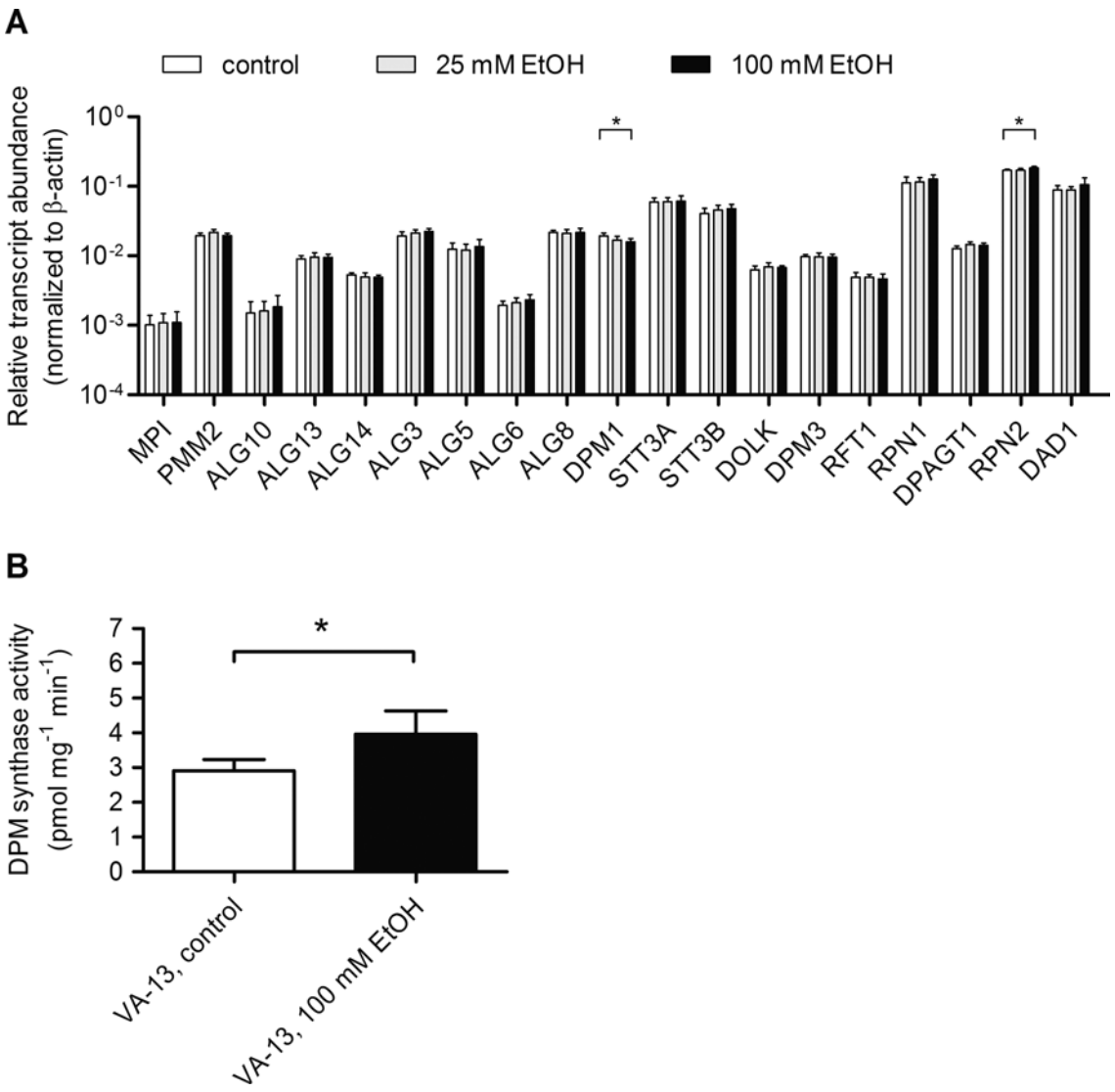

Figure 3

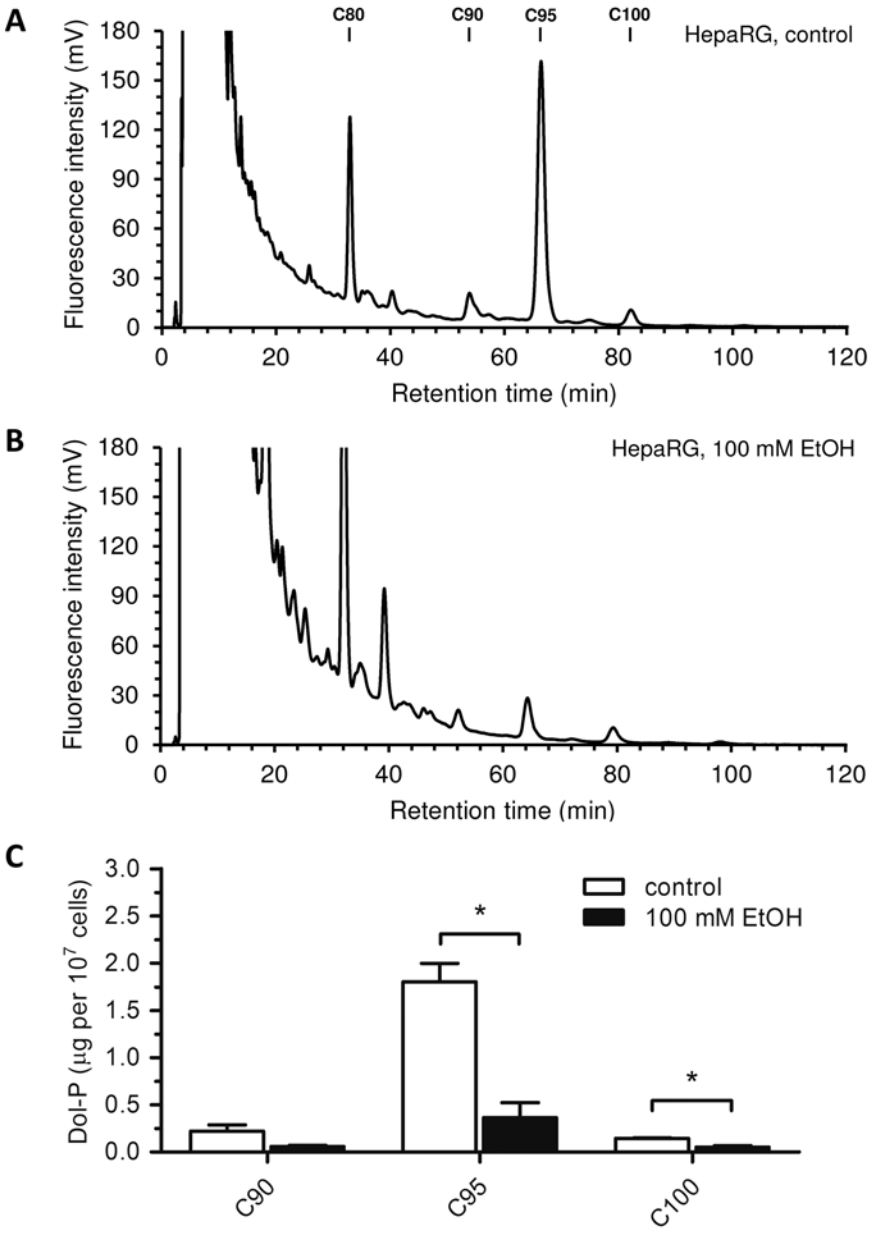

Figure 4

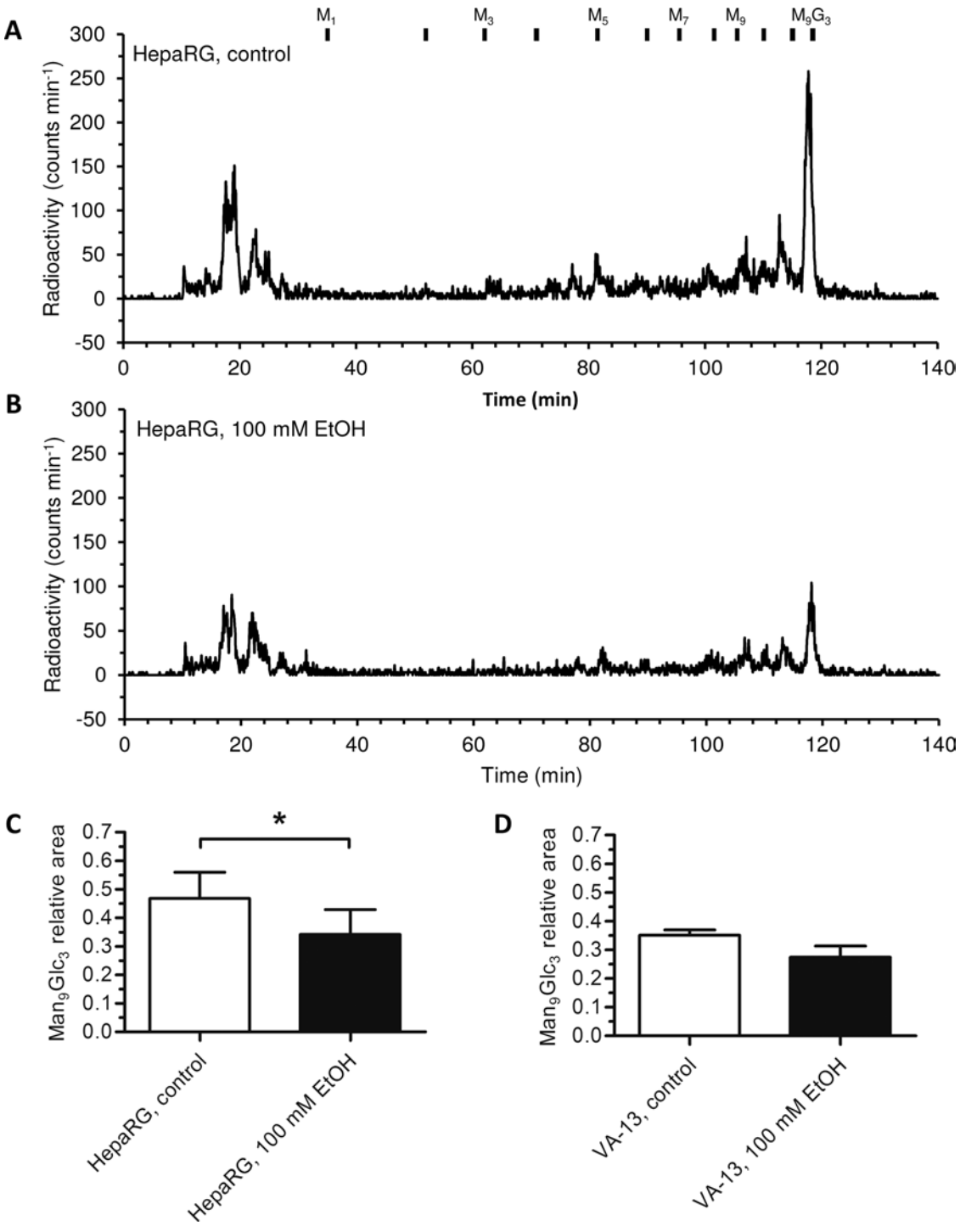

Figure 5